

Search for the decay $B^+ \rightarrow D^{*+} K_S^0$

A. Gritsan,¹ J. P. Alexander,² R. Baker,² C. Bebek,² B. E. Berger,² K. Berkelman,² F. Blanc,² V. Boisvert,² D. G. Cassel,² P. S. Drell,² J. E. Duboscq,² K. M. Ecklund,² R. Ehrlich,² P. Gaidarev,² L. Gibbons,² B. Gittelman,² S. W. Gray,² D. L. Hartill,² B. K. Heltsley,² P. I. Hopman,² L. Hsu,² C. D. Jones,² J. Kandaswamy,² D. L. Kreinick,² M. Lohner,² A. Magerkurth,² T. O. Meyer,² N. B. Mistry,² E. Nordberg,² M. Palmer,² J. R. Patterson,² D. Peterson,² D. Riley,² A. Romano,² J. G. Thayer,² D. Urner,² B. Valant-Spaight,² G. Viehhauser,² A. Warburton,² P. Avery,³ C. Prescott,³ A. I. Rubiera,³ H. Stoeck,³ J. Yelton,³ G. Brandenburg,⁴ A. Ershov,⁴ D. Y.-J. Kim,⁴ R. Wilson,⁴ T. Bergfeld,⁵ B. I. Eisenstein,⁵ J. Ernst,⁵ G. E. Gladding,⁵ G. D. Gollin,⁵ R. M. Hans,⁵ E. Johnson,⁵ I. Karliner,⁵ M. A. Marsh,⁵ C. Plager,⁵ C. Sedlack,⁵ M. Selen,⁵ J. J. Thaler,⁵ J. Williams,⁵ K. W. Edwards,⁶ R. Janicek,⁷ P. M. Patel,⁷ A. J. Sadoff,⁸ R. Ammar,⁹ A. Bean,⁹ D. Besson,⁹ X. Zhao,⁹ S. Anderson,¹⁰ V. V. Frolov,¹⁰ Y. Kubota,¹⁰ S. J. Lee,¹⁰ J. J. O'Neill,¹⁰ R. Poling,¹⁰ T. Riehle,¹⁰ A. Smith,¹⁰ C. J. Stepaniak,¹⁰ J. Urheim,¹⁰ S. Ahmed,¹¹ M. S. Alam,¹¹ S. B. Athar,¹¹ L. Jian,¹¹ L. Ling,¹¹ M. Saleem,¹¹ S. Timm,¹¹ F. Wappler,¹¹ A. Anastassov,¹² E. Eckhart,¹² K. K. Gan,¹² C. Gwon,¹² T. Hart,¹² K. Honscheid,¹² D. Hufnagel,¹² H. Kagan,¹² R. Kass,¹² T. K. Pedlar,¹² H. Schwarzhoff,¹² J. B. Thayer,¹² E. von Toerne,¹² M. M. Zoeller,¹² S. J. Richichi,¹³ H. Severini,¹³ P. Skubic,¹³ A. Undrus,¹³ V. Savinov,¹⁴ S. Chen,¹⁵ J. Fast,¹⁵ J. W. Hinson,¹⁵ J. Lee,¹⁵ D. H. Miller,¹⁵ E. I. Shibata,¹⁵ I. P. J. Shipsey,¹⁵ V. Pavlunin,¹⁵ D. Cronin-Hennessy,¹⁶ A. L. Lyon,¹⁶ E. H. Thorndike,¹⁶ T. E. Coan,¹⁷ V. Fadeyev,¹⁷ Y. S. Gao,¹⁷ Y. Maravin,¹⁷ I. Narsky,¹⁷ R. Stroynowski,¹⁷ J. Ye,¹⁷ T. Wlodek,¹⁷ M. Artuso,¹⁸ C. Boulahouache,¹⁸ K. Bukin,¹⁸ E. Dambasuren,¹⁸ G. Majumder,¹⁸ R. Mountain,¹⁸ S. Schuh,¹⁸ T. Skwarnicki,¹⁸ S. Stone,¹⁸ J. C. Wang,¹⁸ A. Wolf,¹⁸ J. Wu,¹⁸ S. Kopp,¹⁹ M. Kostin,¹⁹ A. H. Mahmood,²⁰ S. E. Csorna,²¹ I. Danko,²¹ K. W. McLean,²¹ Z. Xu,²¹ R. Godang,²² G. Bonvicini,²³ D. Cinabro,²³ M. Dubrovin,²³ S. McGee,²³ G. J. Zhou,²³ A. Bornheim,²⁴ E. Lipeles,²⁴ S. P. Pappas,²⁴ M. Schmidtler,²⁴ A. Shapiro,²⁴ W. M. Sun,²⁴ A. J. Weinstein,²⁴ D. E. Jaffe,²⁵ R. Mahapatra,²⁵ G. Masek,²⁵ H. P. Paar,²⁵ D. M. Asner,²⁶ A. Eppich,²⁶ T. S. Hill,²⁶ R. J. Morrison,²⁶ R. A. Briere,²⁷ G. P. Chen,²⁷ T. Ferguson,²⁷ and H. Vogel²⁷

(CLEO Collaboration)

¹University of Colorado, Boulder, Colorado 80309-0390²Cornell University, Ithaca, New York 14853³University of Florida, Gainesville, Florida 32611⁴Harvard University, Cambridge, Massachusetts 02138⁵University of Illinois, Urbana-Champaign, Illinois 61801⁶Carleton University, Ottawa, Ontario, Canada K1S 5B6 and the Institute of Particle Physics, Canada M5S 1A7⁷McGill University, Montréal, Québec, Canada H3A 2T8 and the Institute of Particle Physics, Canada M5S 1A7⁸Ithaca College, Ithaca, New York 14850⁹University of Kansas, Lawrence, Kansas 66045¹⁰University of Minnesota, Minneapolis, Minnesota 55455¹¹State University of New York at Albany, Albany, New York 12222¹²Ohio State University, Columbus, Ohio 43210¹³University of Oklahoma, Norman, Oklahoma 73019¹⁴University of Pittsburgh, Pittsburgh, Pennsylvania 15260¹⁵Purdue University, West Lafayette, Indiana 47907¹⁶University of Rochester, Rochester, New York 14627¹⁷Southern Methodist University, Dallas, Texas 75275¹⁸Syracuse University, Syracuse, New York 13244¹⁹University of Texas, Austin, Texas 78712²⁰University of Texas - Pan American, Edinburg, Texas 78539²¹Vanderbilt University, Nashville, Tennessee 37235²²Virginia Polytechnic Institute and State University, Blacksburg, Virginia 24061²³Wayne State University, Detroit, Michigan 48202²⁴California Institute of Technology, Pasadena, California 91125²⁵University of California, San Diego, La Jolla, California 92093²⁶University of California, Santa Barbara, California 93106²⁷Carnegie Mellon University, Pittsburgh, Pennsylvania 15213

(Received 14 February 2001; published 4 September 2001)

We report on a search for the decay $B^+ \rightarrow D^{*+} K_S^0$ and its charge conjugate with the CLEO detector at the Cornell Electron Storage Ring (CESR). No candidates are found in 9.10 fb^{-1} of data. The background is estimated to be 0.29 ± 0.05 leading to an upper limit $\mathcal{B}(B^+ \rightarrow D^{*+} K_S^0) = 9.5 \times 10^{-5}$ (90% confidence level).

I. INTRODUCTION

The decay $B^+ \rightarrow D^{*+} K^0$ (throughout this Brief Report charge conjugate decays are implied) is expected to proceed through an annihilation diagram with a W^+ in the s channel with a rate proportional to $|V_{ub}|^2$. Although no calculation exists for the rate of $B^+ \rightarrow D^{*+} K_S^0$, the branching fraction of the related decay $B^+ \rightarrow D^+ K^0$ was estimated [1] to be in the range 0.8×10^{-8} to 3×10^{-6} . The main uncertainty in the calculation arises from the unknown contribution from rescattering of the final state particles. In the reaction $e^+ e^- \rightarrow Y(4S) \rightarrow B^+ B^-$ the B mesons are produced nearly at rest in the laboratory. Therefore the D^{*+} and K_S^0 daughters have large momenta of order of 2.2 GeV/ c essentially in opposite directions. Background events from multibody charm decay and light quark fragmentation generally do not reconstruct to back-to-back D^{*+} and K_S^0 pairs with momenta near 2.2 GeV/ c . Background rejection is further helped by the excellent resolution of the $D^{*+} - D^0$ mass difference and by a reconstruction of the K^0 as a K_S^0 with excellent mass resolution and a significant decay length.

II. DETECTOR AND DATASETS

The CLEO detector [2] is a general purpose detector that provides charged particle tracking, precision electromagnetic calorimetry, charged particle identification, and muon detection. Charged particle detection over 95% of the solid angle is achieved by tracking devices in two different configurations, situated in a magnetic field of 1.5 T. In the first configuration (CLEO II), tracking is provided by three concentric wire chambers, while in the second configuration (CLEO II.V) the innermost wire chamber is replaced by a precision three-layer silicon vertex detector [3]. The momentum resolution is 0.5% at $p=1$ GeV/ c . The drift chambers are surrounded by a time of flight (TOF) system. Energy loss (dE/dx) in the outer drift chamber and the TOF system provide pion-kaon separation. A CsI based electromagnetic calorimeter consisting of a barrel and two endcaps (boundaries at 45° with respect to the beams) has an energy resolution of 4% for 100 MeV electromagnetic showers, and provides π^0 detection. A superconducting coil and muon detectors surround the calorimeter. Redundant triggers provide efficient registration of multiparticle final states.

The Cornell Electron Store Ring (CESR) operates at a center-of-mass energy of approximately 10.6 GeV. The results in this report are based upon 9.10 fb^{-1} of integrated luminosity produced at $e^+ e^-$ center-of-mass energy on the $Y(4S)$. An additional 4.29 fb^{-1} produced 60 MeV below the $B\bar{B}$ threshold provides an estimate of the background due to $e^+ e^- \rightarrow q\bar{q}$, where $q=u,d,s,c$. Hereafter, we refer to these two data samples as “on-4S” and “off-4S” data, respectively. The number of $B\bar{B}$ pairs is $(9.63 \pm 0.19) \times 10^6$.

The Monte Carlo simulation of the CLEO detector is based upon GEANT [4]. Simulated events are processed in the same manner as the data.

III. EVENT RECONSTRUCTION

Charged pion and kaon candidates are selected from tracks that are well reconstructed, consistent with originating from the $e^+ e^-$ interaction point, and not identified as a muon. Particle identification is used to identify charged pions and kaons. The photons used in the π^0 reconstruction are required to have an energy greater than 30 and 50 MeV in the barrel and endcap regions, respectively, and to not be associated with a charged track. The photon-photon invariant mass is required to be within three standard deviations of the known [5] π^0 mass. π^0 are constrained to their known mass and their momentum is required to be greater than 100 MeV/ c . A mass constrained fit is applied to K_S^0 candidates that are formed from oppositely charged pions. The fit is required to have a χ^2 less than 10, improving the resultant K_S^0 momentum resolution by 5% for K_S^0 from D^0 decays while no significant improvement results for K_S^0 from B^+ decays. The K_S^0 candidates are required to originate from the $e^+ e^-$ interaction point and to have a significant decay path (at least three and five standard deviations in the CLEO II and CLEO II.V configurations respectively). The decay path is measured with typical standard deviations of 1.2 mm in CLEO II and 0.7 mm in CLEO II.V.

D^0 candidates are reconstructed in five decay channels: $K^- \pi^+$, $K^- \pi^+ \pi^0$, $K^- \pi^+ \pi^+ \pi^-$, $K_S^0 \pi^+ \pi^-$, and $K_S^0 \pi^+ \pi^- \pi^0$. The charged D^0 daughters are constrained to a common vertex, and the momentum of the D^0 candidate is required to be larger than 1.1 GeV/ c . These D^0 candidates are paired with charged pions to form D^{*+} candidates which are constrained to their known [5] mass, thus improving their momentum resolution by approximately 14%. The D^{*+} candidates are required to have a momentum larger than 1.3 GeV/ c .

IV. EVENT SELECTION

The background is predominantly due to non- $B\bar{B}$ sources so the off-4S data provide a good monitor of the requirements’ effectiveness in rejecting background. Signal event selection requirements are defined using simulated signal events and off-4S data without reference to on-4S data. Signal event selection variables and the corresponding requirements are as follows: $\chi_m^2 \leq 3.5$ [defined in Eq. (1) below], $|\cos \theta_{\text{thr}}| \leq 0.9$ (θ_{thr} is the angle between the thrust axis [6] of the B candidate and the thrust axis of the rest of the event), the normalized second Fox-Wolfram moment [7] ≤ 0.3 , and $|\cos \theta_{\text{hel}}| \geq 0.5$ (θ_{hel} is the helicity angle defined as the angle between the π^+ from D^{*+} decay and the D^{*+} direction in the D^0 rest frame).

χ_m^2 is defined as

$$\chi_m^2 \equiv \left(\frac{m_D - m_D^{\text{nom}}}{\sigma(m_D)} \right)^2 + \left(\frac{\Delta m_{D^{*+}D} - \Delta m_{D^{*+}D}^{\text{nom}}}{\sigma(\Delta m_{D^{*+}D^0})} \right)^2 + \left(\frac{m_{\pi\pi} - m_{K_S^0}^{\text{nom}}}{\sigma(m_{\pi\pi})} \right)^2. \quad (1)$$

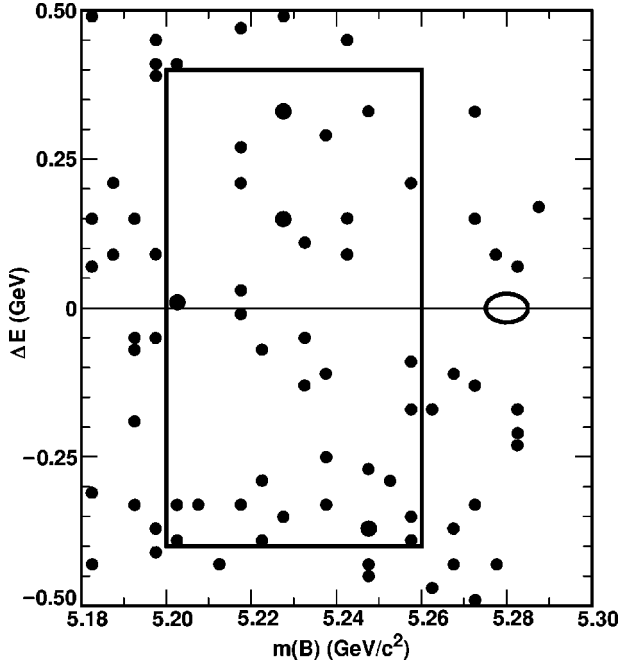


FIG. 1. The ΔE - $m(B)$ distribution for on-4S events. The signal ellipse and the rectangular background region are shown.

Here m_D is the invariant mass of the D^0 candidate, Δm_{D^*D} is the mass difference between the D^{*+} and D^0 candidates, and $m_{\pi\pi}$ is the invariant mass of $\pi^+\pi^-$ pairs that form the K_S^0 candidate; all are calculated from the unconstrained kinematics of the respective final state particles. The same quantities labeled by “nom” are their known [5] values. $\sigma(m_D)$ and $\sigma(\Delta m_{D^*D})$ are the per D^0 decay channel resolutions of m_D and Δm_{D^*D} respectively, and are determined from the data. They are approximately 6 and 0.53 MeV/ c^2 respectively. The efficiency of the four requirements is 34% and their background rejection factor is 82. If an event has more than one $B^+ \rightarrow D^{*+} K_S^0$ candidate, the candidate with the lowest χ_m^2 is chosen.

V. RESULTS

Results are presented in a two-dimensional plot of the energy difference ΔE and the beam-constrained mass $m(B)$ (see Fig. 1), with $\Delta E = E_{D^{*+}} + E_{K_S^0} - E_{\text{beam}}$ and $m(B) = \sqrt{E_{\text{beam}}^2 - (\mathbf{p}_{D^{*+}} + \mathbf{p}_{K_S^0})^2}$. Here $E_{D^{*+}}$, $E_{K_S^0}$, $\mathbf{p}_{D^{*+}}$, and $\mathbf{p}_{K_S^0}$ are the mass-constrained energy and momentum of D^{*+} and K_S^0 respectively. The resolution in ΔE is 11.9 MeV and in $m(B)$ it is 2.5 MeV/ c^2 , the latter dominated by the spread in beam energy. The signal region is enclosed by an ellipse with semiaxes of length 24 MeV along ΔE and 5 MeV/ c^2 along $m(B)$, with an efficiency of 82%. There are no events in the signal region. The background in the signal region is estimated from the number of events that are in the rectangular region shown in Fig. 1, defined by $|\Delta E| < 0.4$ GeV and $5.2 \leq m(B) \leq 5.26$ GeV/ c^2 . The 37 events in this region are

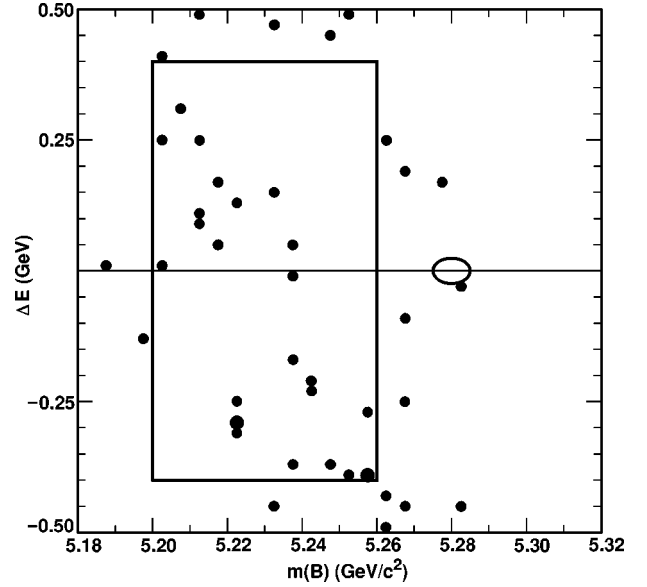


FIG. 2. The ΔE - $m(B)$ distribution for off-4S events. The signal ellipse and the rectangular background region are shown.

scaled by the ratio of areas of the signal and background region to give a background estimate of 0.29 ± 0.05 events.

In Fig. 2 we show the ΔE - $m(B)$ distribution for off-4S events. Here the calculated value of $m(B)$ is increased by 30 MeV/ c^2 to take into account the lower center-of-mass energy of the off-4S data. There are no signal events in the signal region and 25 events in the background region. To compare with the 37 events found in the on-4S data, the 25 events must be scaled by the ratio of luminosities in the on-4S and off-4S data, and the ratio of the center-of-mass energy squared to obtain 50.1 ± 10.0 . This number is larger than but consistent with the 37 events in the background region in on-4S data, and shows that the background is predominantly from non- $B\bar{B}$ sources.

Based upon an acceptance (including all branching fractions) of 2.76×10^{-3} and the number of $B\bar{B}$ pairs, one signal event corresponds to $\mathcal{B}(B^+ \rightarrow D^{*+} K^0) = 3.7 \times 10^{-5}$. Here we assumed an equal production of neutral and charged B pairs from $Y(4S)$ decays, consistent [8] with experiment. The observation of zero events in the signal ellipse with an expectation of 0.29 events from background corresponds [9] to a 90% confidence level (C.L.) upper limit on the number of signal events of 2.15 and a 90% C.L. upper limit on the branching fraction of $\mathcal{B}(B^+ \rightarrow D^{*+} K^0) = 8.0 \times 10^{-5}$.

Systematic uncertainties originate from track finding (1% per track, 5% per soft pion from D^{*+} decay), dE/dx (2% per track), K_S^0 finding (3% per K_S^0), π^0 finding (5.5% per π^0), the number of produced $B\bar{B}$ (2%), and the five D^0 branching fractions (2.0-5.2% [5] for the three dominant D^0 decay channels $K^-\pi^+$, $K^-\pi^+\pi^0$, $K^-\pi^+\pi^+\pi^-$). The weighted average systematic uncertainty is 10%. The 16% statistical uncertainty in the background estimate is added to

obtain a total uncertainty on the background estimate of 19%. This leads to a 90% C.L. upper limit $\mathcal{B}(B^+ \rightarrow D^{*+} K^0) = 9.5 \times 10^{-5}$.

VI. SUMMARY AND CONCLUSION

We have searched for the decay $B^+ \rightarrow D^{*+} K_S^0$. In a data sample with 9.10-fb^{-1} integrated luminosity, corresponding to 9.63×10^6 produced $B\bar{B}$ pairs, we found zero signal events on an estimated background of 0.29 ± 0.05 . Including systematic uncertainties, we find an upper limit $\mathcal{B}(B^+ \rightarrow D^{*+} K^0) = 9.5 \times 10^{-5}$ (90% C.L.).

ACKNOWLEDGMENTS

We gratefully acknowledge the effort of the CESR staff in providing us with excellent luminosity and running conditions. M.S. thanks the PFF program of the NSF and the Research Corporation, A.H.M. thanks the Texas Advanced Research Program, F.B. thanks the Swiss National Science Foundation, and E.v.T. thanks the Alexander von Humboldt Stiftung for support. This work was supported by the National Science Foundation, the U.S. Department of Energy, and the Natural Sciences and Engineering Research Council of Canada.

-
- [1] Z.-Z. Xing, Phys. Rev. D **53**, 2847 (1996).
[2] CLEO Collaboration, Y. Kubota *et al.*, Nucl. Instrum. Methods Phys. Res. A **320**, 66 (1992).
[3] T. Hill, Nucl. Instrum. Methods Phys. Res. A **418**, 32 (1998).
[4] R. Brun *et al.*, CERN DD/EE/84-1.
[5] Particle Data Group, D. E. Groom *et al.*, Eur. Phys. J. C **15**, 1 (2000).
[6] E. Farhi, Phys. Rev. Lett. **39**, 1587 (1977).
[7] G. C. Fox and S. Wolfram, Nucl. Phys. **B149**, 413 (1979).
[8] CLEO Collaboration, J. P. Alexander *et al.*, Phys. Rev. Lett. **86**, 2737 (2001).
[9] G. Feldman and R. Cousins, Phys. Rev. D **57**, 3873 (1998).